

2D Stability Selection: Design Jittering for Doubly Stable Feature Selection

Mahdi Nourai^{1*}, Houying Zhu¹ and Samuel Muller^{1,2}

¹School of Mathematical and Physical Sciences, Macquarie University, Sydney, 2109, NSW, Australia.

²School of Mathematics and Statistics, The University of Sydney, Sydney, 2006, NSW, Australia.

*Corresponding author(s). E-mail(s): soheil.nourai@mq.edu.au;

Abstract

We study feature selection in high-dimensional regression under two distinct sources of instability: sampling variability and measurement error in the design matrix. Stability Selection addresses the former through sub-sampling and aggregation, but does not explicitly stress-test robustness to noisy predictors. We introduce doubly stable feature selection, a perturb-and-aggregate framework that targets features whose inclusion is stable both across randomization and across increasing levels of design noise. The method injects controlled additive noise into the design matrix, fits a fixed base selector such as the Lasso on the perturbed data, and aggregates selection frequencies. Sweeping over a grid of noise levels yields a stability path that summarizes robustness to measurement error while using the full sample size and isolating the effect of design perturbations. On the theory side, we show that classical model-selection conditions are preserved under sufficiently small perturbations, with a high-probability extension for Gaussian noise. Empirically, experiments on synthetic and real datasets show improved robustness compared with Stability Selection and standard base selectors.

Keywords: Feature Selection, High-Dimensional Regression, Measurement Error, Perturbation-Based Methods, Stability Selection, Variable Selection

1 Introduction

1.1 Problem and Perspective

Estimating discrete structures and selecting relevant features are central tasks in machine learning, bioinformatics, and statistics. In high-dimensional regimes, the usefulness of a selected model depends critically on its *stability* (Meinshausen and Bühlmann, 2010; Müller and Welsh, 2010). Unstable selections are difficult to reproduce and often fail to generalize. This has led to a substantial literature on stability in feature selection and related problems (Meinshausen and Bühlmann, 2010; Shah and Samworth, 2013; Nogueira et al., 2018; Wang et al., 2018; Soloff et al., 2024; Nourai et al., 2026), as well as work on learning invariant structure under distributional shifts (Shen et al., 2020; Zhang et al., 2021; Cui and Athey, 2022). Two distinct sources drive instability. The first is *sampling variability*: different samples from the same distribution can yield different selected sets (Meinshausen and Bühlmann, 2010; Shah and Samworth, 2013; Faletto and Bien, 2022). The second is *measurement error* in the predictors, where the effective design varies due to noisy acquisition, leading to an errors-in-variables setting (Nghiem et al., 2020; Nghiem and Potgieter, 2023; Liu and Nghiem, 2026). These sources are typically studied separately. We consider linear regression with fixed design, $Y = X\beta + \varepsilon$, where $X \in \mathbb{R}^{n \times p}$ is centered and scaled, $\mathbb{E}(\varepsilon|X) = 0$, and $\text{Var}(\varepsilon|X) = \sigma^2 I_n$. Our goal is to study feature selection procedures under *both* sampling variability and perturbations of the design.

1.2 Doubly Stable Feature Selection

We introduce *doubly stable feature selection*, which enforces stability along two axes: (i) stability across randomized realizations at a fixed noise level, and (ii) stability as the level of measurement error increases. Given a base selector, such as the Least Absolute Shrinkage and Selection Operator (Lasso; Tibshirani, 1996), the Elastic Net (ENet; Zou and Hastie, 2005), or the Smoothly Clipped Absolute Deviation penalty (SCAD; Fan and Li, 2001), we repeatedly perturb the design matrix via $X^{(\delta)} = X + W$, where W injects controlled noise with variance δ^2 , and aggregate selections across B randomized realizations at fixed δ . This yields selection frequencies that quantify stability under a fixed perturbation level. We then track these frequencies along a grid of increasing δ , producing a *noise path* that reveals how selections degrade under increasing measurement error. This construction generalizes Stability Selection (Meinshausen and Bühlmann, 2010) by introducing a second axis: instead of varying sub-samples or penalties, we vary the magnitude of perturbations applied directly to the design. The proposed framework has three main properties. First, it is *method-agnostic*: it applies to any selection procedure satisfying mild regularity conditions. Second, it preserves the full sample size n , unlike sub-sampling-based approaches such as Stability Selection. Third, it yields a diagnostic analogous to a regularization path: instead of tracking solutions over λ , we track selection frequencies over δ , exposing robustness to measurement error.

1.3 Motivating Example

We illustrate this effect in a synthetic experiment with $n = 100$ and $p = 1,000$, where five predictors are relevant with coefficients 5, 4, 3, 2, 1. The relevant predictors follow a compound symmetric correlation structure with $\rho_{\text{rel}} = 0.5$, while irrelevant predictors follow a compound symmetric structure with $\rho_{\text{irr}} = 0.1$. Cross-correlations are controlled by $\rho_{\text{mix}} \in \{0.001, 0.5, 0.9\}$. The response is generated as $Y = X\beta + \varepsilon$ with $\varepsilon \sim \mathcal{N}(0, I_n)$. To model increasing feature noise, we consider perturbations $X^{(\delta)} = X + W$ with $W_{ik} \sim \mathcal{N}(0, \delta^2)$ over a grid $\delta \in [0.01, 5]$. For each δ , we generate $B = 100$ realizations and compute selection frequencies using Lasso, ENet, and SCAD with fixed tuning parameters. Figure 1 shows the results for the Lasso; the ENet and SCAD results are reported in the appendix. At low noise levels, irrelevant predictors can attain high selection frequencies, yielding false discoveries. As δ increases, these frequencies decay and separation between relevant and irrelevant predictors emerges. For large δ , all frequencies collapse toward zero. This pattern is consistent across methods and correlation regimes. These observations motivate selecting features based on their persistence along the noise path, rather than at a single noise level.

1.4 Related Work

Randomization and perturbation are widely used to stabilize learning procedures, including Stability Selection (Meinshausen and Bühlmann, 2010), the Randomized Lasso (Meinshausen and Bühlmann, 2010), the Jackknife (Wu, 1986), Random Forests (Breiman, 2001), and Random-Projection Ensemble Classification (Cannings and Samworth, 2017). Our approach differs in that perturbations are applied directly to the design to model measurement error, rather than to resampling or parameter randomization. The perspective is also related to invariance-based methods that seek stable structure across environments (Pfister et al., 2021; Jeong and Rothenhäusler, 2025; Shen et al., 2026).

Section 2 presents the proposed methodology and theoretical results. Section 3 reports empirical evaluations on synthetic and real datasets. Section 4 concludes with a discussion of limitations and directions for future work. All remarks and proofs are deferred to the appendix.

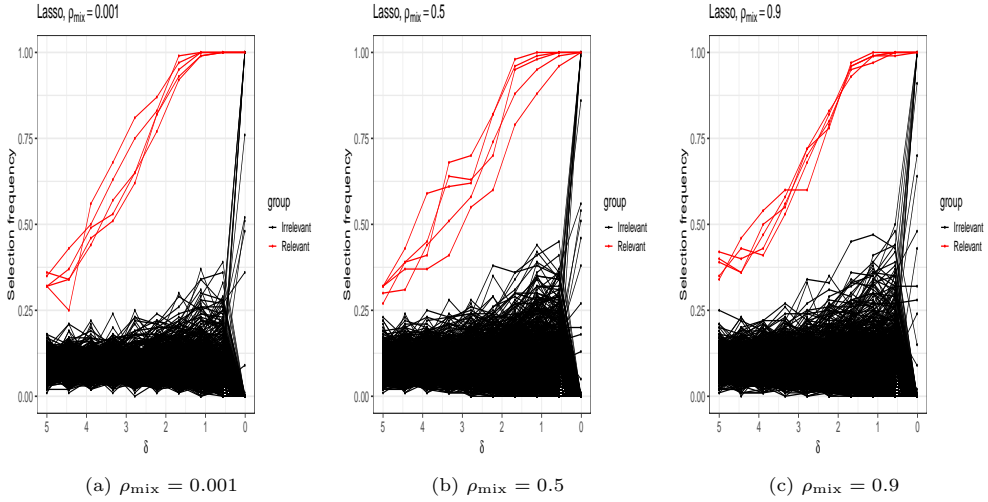


Fig. 1: Selection frequency of relevant (red) and irrelevant (black) features for Lasso under increasing design noise level δ

2 Methodology

2.1 Lasso Setup and Small-Perturbation Robustness

We work in the linear regression setting of Section 1 and use the Lasso as our running example. Background material on the Lasso and the perturbation algebra is provided in the appendix. For the Lasso, exact support recovery is typically established under the Irrepresentable Condition (IC) and a minimum signal condition, together with a choice of λ in an appropriate range (Zhao and Yu, 2006; Meinshausen and Bühlmann, 2006; Bühlmann and Van De Geer, 2011). The IC can be stated as follows. Let $\Sigma \in \mathbb{R}^{p \times p}$ be a Gram matrix, i.e., $\Sigma = \frac{1}{n} X^\top X$, and let $S \subset \{1, \dots, p\}$ be the active set and S^c its complement. Suppose Σ_{SS} , the sub-matrix of Σ indexed by S , is invertible and

$$\|\Sigma_{S^c S} \Sigma_{SS}^{-1}\|_\infty \leq 1 - \eta,$$

for some $\eta \in (0, 1)$. This condition constrains the dependence between relevant and irrelevant features relative to the dependence within the relevant set.

Lemma 1 (Small perturbation preserves irrepresentability) *Let $S \subset \{1, \dots, p\}$ denote the active set and suppose Σ_{SS} is invertible. Assume the IC holds for Σ , $\|\Sigma_{S^c S} \Sigma_{SS}^{-1}\|_\infty \leq 1 - \eta$, for some $\eta \in (0, 1)$. Let $\Sigma^{(\delta)} = \Sigma + \Delta$ satisfy $\|\Delta\|_\infty \leq C_1 \delta + C_2 \delta^2$, for some $C_1, C_2 > 0$. Then there exists $\delta_0 = \delta_0(\Sigma_{SS}, C_1, C_2, \eta) > 0$ such that for all $0 \leq \delta \leq \delta_0$, $\Sigma_{SS}^{(\delta)}$ is invertible and*

$$\left\| \Sigma_{S^c S}^{(\delta)} (\Sigma_{SS}^{(\delta)})^{-1} \right\|_\infty \leq 1 - \frac{\eta}{2}.$$

Consequently, the IC continues to hold under perturbation with a reduced margin $1 - \tilde{\eta}$ for some $\tilde{\eta} \in (0, \eta)$ depending on Σ_{SS} and the perturbation constants.

Proof is shown in the appendix. Therefore, Lemma 1 implies that if the original design satisfies the IC, then this property is preserved under sufficiently small additive perturbations. We next extend this deterministic statement to a probabilistic setting by modeling the additive measurement noise as Gaussian, and derive a high-probability analog of Lemma 1. The deterministic assumption $\|\Delta\|_\infty \leq C\delta$ serves as an envelope for the stochastic regime. In the Gaussian setting of Section 2.2, we obtain with high probability a bound of the form $\|\Delta\|_\infty \leq \varepsilon$, where $\varepsilon = p(t_1 + t_2)$. In the sequel, we invoke Lemma 1 with $C\delta$ replaced by ε , i.e., treating ε as the effective perturbation size.

2.2 Gaussian Perturbations and High-Probability Robustness

In this section, we extend the results of Section 2.1 to a probabilistic setting by considering Gaussian perturbations of X . We apply Lemma 1 with $\Sigma^{(\delta)}$ replaced by the centered matrix $\tilde{\Sigma}^{(\delta)}$, since the lemma only requires a bound on $\|\Delta\|_\infty$, where $\Delta = \tilde{\Sigma}^{(\delta)} - \Sigma$.

Theorem 1 (Gaussian perturbations preserve irrepresentability with high probability) *Fix a deterministic design matrix $X \in \mathbb{R}^{n \times p}$ and let $X^{(\delta)} = X + W$, and $W_{ik} \stackrel{iid}{\sim} \mathcal{N}(0, \delta^2)$. Define $\Sigma = \frac{1}{n} X^\top X$, and $\tilde{\Sigma}^{(\delta)} = \frac{1}{n} (X^{(\delta)})^\top X^{(\delta)} - \delta^2 I_p$. Assume $\frac{1}{n} \sum_{i=1}^n X_{ij}^2 \leq M^2$ for all j . Let S be the active set and suppose $\|\Sigma_{S^c S} \Sigma_{SS}^{-1}\|_\infty \leq 1 - \eta$, for $\eta \in (0, 1)$. Let $\alpha \in (0, 1)$, and let δ be such that $\varepsilon := p(t_1 + t_2) \leq \varepsilon_0$, where $\varepsilon_0 = \varepsilon_0(\Sigma_{SS}, \eta)$ is any constant small enough so that Lemma 1 applies with $\|\Delta\|_\infty \leq \varepsilon_0$. Then, under the above conditions,*

$$\mathbb{P}\left(\left\|\tilde{\Sigma}_{S^c S}^{(\delta)} (\tilde{\Sigma}_{SS}^{(\delta)})^{-1}\right\|_\infty \leq 1 - \frac{\eta}{2}\right) \geq 1 - \alpha.$$

Proof is provided in the appendix, together with Lemma 2, which is used in the proof. Although the IC is a classical consistency condition for Lasso model-selection consistency, closely related “near-orthogonality” assumptions between active and inactive features also arise in other selection procedures (e.g., forward selection; [Wieczorek and Lei \(2022\)](#)). Moreover, even methods designed for correlated designs typically require consistency conditions of a similar flavor (see, for instance, [Wang et al. \(2018\)](#) and [Takada et al. \(2018\)](#)).

We now turn to larger perturbations. Figure 1 suggests that, given a fixed λ , as the noise level increases, the selection frequencies of all features decrease. Remark 2 (in the appendix) indicates that for large δ , the induced errors-in-variables effect can overwhelm the signal, leading to vanishing selection frequencies for all features. From a stability perspective, performing bagging at each noise level δ improves stability with respect to random sampling at the corresponding perturbation magnitude ([Meinshausen and Bühlmann, 2010](#); [Soloff et al., 2024](#)). We additionally consider a second notion of stability, namely robustness to measurement error, by selecting features under a more stringent measurement-error stress test. Motivated by the empirical

results in Figure 1, we propose an additional layer of bagging over measurement error to further promote stability under this criterion.

2.3 δ -Averaged Selection Frequencies and Support Recovery

Motivated by Figure 1, we move beyond the small- δ regime and study how selection behaves along a path of increasing measurement noise. Fix a tuning parameter λ that does not depend on δ , and for each perturbation level $\delta \geq 0$ consider the perturbed design $X^{(\delta)} = X + W$ with $W_{ik} \stackrel{\text{iid}}{\sim} \mathcal{N}(0, \delta^2)$. Let $\hat{\beta}^{(\delta)} = \hat{\beta}^{(\delta)}(\lambda)$ denote the fitted coefficient vector obtained by applying the chosen selector to $(X^{(\delta)}, Y)$.

We quantify stability with respect to measurement error via selection frequencies. Treating (X, Y) as fixed throughout, define for each feature j and perturbation level δ the population selection frequency $f_j^{(\delta)} := \mathbb{P}(\hat{\beta}_j^{(\delta)} \neq 0)$, where the probability is over W (and any algorithmic randomness). In practice, we approximate $f_j^{(\delta)}$ by Monte Carlo bagging: for each δ , generate i.i.d. perturbations $\{W^{(b)}\}_{b=1}^B$ with entries $\mathcal{N}(0, \delta^2)$, fit the selector on $(X + W^{(b)}, Y)$, and form the empirical frequency $\hat{f}_j^{(\delta)} := \frac{1}{B} \sum_{b=1}^B 1\{\hat{\beta}_j^{(b, \delta)} \neq 0\}$.

Averaging over δ

Figure 1 and Remark 2 suggest that, as δ increases, selection frequencies tend to decrease, with a potentially informative intermediate range in which relevant and irrelevant features are still separable by their frequencies. To exploit robustness across noise magnitudes, we aggregate frequencies across a finite grid $\mathcal{G} = \{\delta_1, \dots, \delta_m\} \subset [0, \infty)$ by the delta-averaged population and empirical frequencies $\bar{f}_j := \frac{1}{m} \sum_{\delta \in \mathcal{G}} f_j^{(\delta)}$, and $\hat{\bar{f}}_j := \frac{1}{m} \sum_{\delta \in \mathcal{G}} \hat{f}_j^{(\delta)}$. This averaging step rewards features that are selected consistently across perturbation magnitudes and reduces sensitivity to the choice of any single δ .

We now state a minimal condition under which thresholding the averaged empirical frequencies recovers the true active set S .

Assumption 1 (Separation of δ -averaged selection frequencies). *Let $S \subset \{1, \dots, p\}$ denote the active set and S^c its complement. For a given grid of perturbation levels $\mathcal{G} = \{\delta_1, \dots, \delta_m\}$, define \bar{f}_j as the selection frequency of feature j averaged over all levels in \mathcal{G} . We require that there exists a constant $\gamma > 0$ such that $\min_{j \in S} \bar{f}_j \geq \max_{k \in S^c} \bar{f}_k + \gamma$.*

Assumption 1 is a frequency-domain analog of classical separability conditions in model selection. It requires that every active feature is selected more frequently, on average across perturbation levels in \mathcal{G} , than every inactive feature, with a strictly positive gap γ separating the two groups. Intuitively, this acts as a clean score threshold: across perturbation scales, active features consistently score higher than inactive ones by at least γ . This separation is what enables reliable variable selection. In applications, \mathcal{G} is chosen to cover a range of perturbation magnitudes that is large enough to stress-test robustness yet not so large that all frequencies collapse toward zero (see, Remark 2).

We now state a model-agnostic recovery guarantee: under Assumption 1, thresholding the delta-averaged empirical selection frequencies recovers the true support S with high probability.

Theorem 2 (Support recovery from δ -averaged empirical frequencies) *Assume Assumption 1 holds with margin $\gamma > 0$. Let $\alpha \in (0, 1)$, where $m = |\mathcal{G}|$ is the number of perturbation levels and B is the number of design realizations generated at each perturbation level. Define $\varepsilon := \sqrt{\frac{\log(2mp/\alpha)}{2B}}$. Then, with probability at least $1 - \alpha$ over the perturbations used to compute $\{\hat{f}_j^{(\delta)}\}_{\delta \in \mathcal{G}, 1 \leq j \leq p}$,*

$$\min_{j \in S} \hat{f}_j \geq \max_{k \in S^c} \hat{f}_k + (\gamma - 2\varepsilon).$$

In particular, if $\varepsilon < \gamma/2$, then there exists a threshold τ such that

$$\hat{S}(\tau) := \{j : \hat{f}_j \geq \tau\} = S.$$

Proof is shown in the appendix. Theorem 2 provides a formal guarantee that the proposed procedure achieves exact support recovery with high probability under a quantifiable error budget. The empirical separation between active and inactive features is preserved up to the deviation term 2ε , ensuring that the ordering induced by the δ -averaged frequencies remains stable. In particular, exact recovery is possible when the stochastic error is sufficiently small relative to the margin γ , i.e., $\varepsilon < \gamma/2$. Moreover, the bound shows that the error decreases as B increases, reflecting improved accuracy with additional Monte Carlo sampling across perturbations and design realizations.

Thresholding by Estimated Model Size

Since the true model size $s = |S|$ is unknown in practice, we estimate s by locating the largest drop in the sorted δ -averaged empirical frequencies, following Huang et al. (2026). Under the separation guarantee of Theorem 2, the averaged frequencies admit a strict partition: with high probability, all $j \in S$ have larger \hat{f}_j than all $k \in S^c$. Consequently, the sorted sequence $\hat{f}_{(1)} \geq \dots \geq \hat{f}_{(p)}$ exhibits a pronounced drop at the boundary between the two groups. This motivates estimating the split point by the largest adjacent gap and using the midpoint between the two neighboring values as a data-driven threshold. We define

$$\hat{s} := \arg \max_{1 \leq k < p} (\hat{f}_{(k)} - \hat{f}_{(k+1)}), \quad \hat{\tau} := \frac{1}{2}(\hat{f}_{(\hat{s})} + \hat{f}_{(\hat{s}+1)}), \quad \hat{S} := \{j : \hat{f}_j \geq \hat{\tau}\}.$$

We summarize the full procedure in Algorithm 1 in the appendix.

3 Numerical Results

Synthetic Data

We conduct a Monte Carlo simulation with $n_{\text{rep}} = 200$ independent replications in a high-dimensional setting with training sample size $n = 100$ and $p = 1,000$ features. The true active set is $S = \{200, 400, 600, 800, 1000\}$, with coefficients $\beta_j \in \{5, 4, 3, 2, 1\}$ on S (in that order) and $\beta_j = 0$ otherwise. For each replication, we generate a latent design $X_0 \in \mathbb{R}^{n \times p}$ from a centered multivariate normal distribution with a structured covariance matrix: correlations among relevant features are set to $\rho_{\text{rel}} = 0.5$, among irrelevant features to $\rho_{\text{irr}} = 0.05$, and between relevant and irrelevant features to $\rho_{\text{mix}} = 0.4$, followed by projection to the nearest positive definite matrix. The resulting design is standardized by centering and scaling each column using its empirical mean and standard deviation.

To model measurement error in the covariates, we observe $X = X_0 + W$, where $W_{ik} \stackrel{\text{iid}}{\sim} \mathcal{N}(0, \delta_{\text{obs}}^2)$ and $\delta_{\text{obs}} \in \{0, 0.5, 1, 1.5, 2\}$. The response is generated from the latent design, $y = X_0\beta + \varepsilon$, where $\varepsilon \sim \mathcal{N}(0, I_n)$, so that perturbations affect only the observed predictors.

For each δ_{obs} and replication, we fit (i) the Lasso and (ii) ENet with $\alpha = 1$ and $\alpha = 0.5$, respectively, using a fixed regularization level $\lambda = \sqrt{\log(p)/n}$. We further consider Stability Selection based on half-sample sub-sampling with $B = 100$ resamples and thresholds $\tau \in \{0.6, 0.7, 0.8, 0.9\}$ for both models. Finally, we apply our jitter-based procedure that adds Gaussian perturbations over a grid $\delta \in \{0.05, \dots, 2.5\}$ (10 equispaced values), with $B = 100$ perturbations per grid point, selecting the top $|S| = 5$ features according to averaged selection frequencies (oracle model size). In the next experiment, we use the data-driven variant of our method.

Performance is evaluated using the F1 score for support recovery and a selection stability measure computed from binary selection matrices across replications (Nogueira et al., 2018). The simulation is implemented in R and executed on a MacBook Air 13-inch with parallelization over 7 cores.

In the oracle setting (Table 1, left panel), performance degrades monotonically as δ_{obs} increases, consistent with measurement-error effects. At $\delta_{\text{obs}} = 0$, all aggregation-based methods achieve near-perfect recovery, while Lasso and ENet fail substantially ($\text{F1} \leq 0.50$), indicating that aggregation alone suffices in the noise-free regime. At $\delta_{\text{obs}} = 0.5$, Stability Selection remains strong ($\text{F1} \approx 0.95\text{--}0.99$), but jitter attains perfect recovery, while single-fit methods collapse. At $\delta_{\text{obs}} = 1$, jitter is best (0.94/0.97). Stability Selection becomes threshold-sensitive, with intermediate thresholds performing best and high thresholds degrading. For $\delta_{\text{obs}} \geq 1.5$, all methods deteriorate sharply. Jitter remains most robust, achieving the highest or near-highest F1 across high-noise regimes, while Stability Selection and single-fit estimators collapse.

In the data-driven setting (Table 1, right panel), the largest-gap rule closely matches the oracle benchmark in the low-noise regime. For $\delta_{\text{obs}} \leq 0.5$, jitter attains perfect recovery ($\text{F1} = 1.00$) and maximal stability, while standard Lasso and ENet remain poor, confirming that the gain is driven by aggregation rather than oracle tuning. At $\delta_{\text{obs}} = 1$, performance begins to separate: jitter remains competitive

(0.87/0.93), but no longer dominates the best stability-selection variants, indicating the onset of model-size estimation error. For $\delta_{\text{obs}} \geq 1.5$, all methods deteriorate sharply. The main failure mode for jitter is threshold estimation becoming unstable as averaged selection frequencies flatten and the largest-gap signal weakens. In this regime, Stability Selection, especially lower-threshold variants often achieves higher F1 and comparable or better stability. Overall, the data-driven results show that δ -averaging remains effective without oracle information, and that robustness at high noise is primarily limited by size-threshold estimation.

Affymetrix Rat Genome 230 2.0 Array

As a real-world example, we investigate ‘Affymetrix Rat Genome 230 2.0 Array’ microarray data introduced by [Scheetz et al. \(2006\)](#). This dataset comprises $n = 120$ twelve-week-old male rats, with expression levels recorded for nearly 32,000 gene probes for each rat. The primary objective of this analysis is to identify the probes most strongly associated with the expression level of the TRIM32 probe (`1389163_at`), which has been linked to the development of Bardet-Biedl syndrome ([Chiang et al., 2006](#)). This genetically heterogeneous disorder affects multiple organ systems, including the retina. In accordance with the pre-processing steps outlined by [Huang et al. \(2008\)](#), we excluded gene probes with a maximum expression level below the 25th percentile and those exhibiting an expression range smaller than 2. This filtering process yielded a refined set of $p = 3,083$ gene probes that demonstrated sufficient expression and variability for further analysis.

With $\lambda = \lambda_{1\text{se}}$ chosen by cross-validation, the data-driven jitter procedure estimated $\hat{\tau} = 0.406$ and selected four probes (`1376747_at`, `1389457_at`, `1390539_at`, `1392982_at`), whereas sub-sampling-based Stability Selection with the Lasso at the same λ selected none even with the most permissive decision threshold, that is, 0.6 (and likewise none when using $\lambda/2$). Although a fully correct Stability Selection analysis is typically performed over a grid of λ values, it is also practically important to assess stability for a single carefully tuned model, as done here by fixing λ via cross-validation.

4 Conclusion

We proposed a general framework for feature selection that is stable to both sampling variability and measurement error. The framework is model-agnostic, as supported by our empirical results, while our theoretical analysis focuses on the Lasso to characterize how small injected perturbations affect selection and to clarify when robustness can be expected. Several directions remain open. First, we analyzed additive Gaussian perturbations; extending the theory and practice to non-Gaussian noise (e.g., heavy-tailed or correlated) and to alternative error mechanisms beyond additivity is an important next step. Second, our procedure depends on an estimate of the true model size, and performance degrades when this quantity is misspecified. Developing more accurate and broadly applicable strategies for estimating the model size, ideally with finite-sample guarantees, is a key avenue for future work.

Table 1: Stability and F1 across $\delta_{\text{obs}} \in \{0, 0.5, 1.0, 1.5, 2.0\}$. Left panel: oracle variant. Right panel: data-driven variant. Bold indicates the maximum within each δ_{obs} separately for Stability and F1 within each panel.

δ_{obs}	Oracle			Data-driven	
	Method	Stability	F1	Stability	F1
0.0	Lasso	0.32	0.50	0.32	0.50
0.0	ENet	0.11	0.18	0.11	0.18
0.0	StabL_0.6	0.99	1.00	0.99	1.00
0.0	StabL_0.7	1.00	1.00	1.00	1.00
0.0	StabL_0.8	1.00	1.00	1.00	1.00
0.0	StabL_0.9	1.00	1.00	1.00	1.00
0.0	StabEN_0.6	0.92	0.96	0.93	0.97
0.0	StabEN_0.7	0.98	0.99	0.98	0.99
0.0	StabEN_0.8	1.00	1.00	1.00	1.00
0.0	StabEN_0.9	1.00	1.00	1.00	1.00
0.0	Jitter	1.00	1.00	1.00	1.00
0.5	Lasso	0.11	0.13	0.11	0.13
0.5	ENet	0.12	0.10	0.11	0.10
0.5	StabL_0.6	0.91	0.96	0.91	0.95
0.5	StabL_0.7	0.97	0.98	0.98	0.99
0.5	StabL_0.8	0.98	0.99	0.97	0.98
0.5	StabL_0.9	0.94	0.96	0.94	0.96
0.5	StabEN_0.6	0.82	0.91	0.83	0.92
0.5	StabEN_0.7	0.95	0.98	0.96	0.98
0.5	StabEN_0.8	0.99	0.99	0.99	1.00
0.5	StabEN_0.9	0.98	0.99	0.98	0.99
0.5	Jitter	1.00	1.00	1.00	1.00
1.0	Lasso	0.11	0.10	0.11	0.10
1.0	ENet	0.11	0.09	0.11	0.09
1.0	StabL_0.6	0.83	0.91	0.82	0.91
1.0	StabL_0.7	0.88	0.93	0.88	0.94
1.0	StabL_0.8	0.84	0.90	0.83	0.89
1.0	StabL_0.9	0.68	0.78	0.67	0.76
1.0	StabEN_0.6	0.73	0.85	0.73	0.85
1.0	StabEN_0.7	0.86	0.93	0.87	0.93
1.0	StabEN_0.8	0.88	0.93	0.89	0.94
1.0	StabEN_0.9	0.80	0.87	0.78	0.86
1.0	Jitter	0.94	0.97	0.87	0.93
1.5	Lasso	0.09	0.09	0.09	0.09
1.5	ENet	0.09	0.08	0.08	0.08
1.5	StabL_0.6	0.58	0.76	0.57	0.75
1.5	StabL_0.7	0.57	0.72	0.54	0.70
1.5	StabL_0.8	0.44	0.59	0.44	0.59
1.5	StabL_0.9	0.24	0.34	0.26	0.35
1.5	StabEN_0.6	0.55	0.74	0.54	0.73
1.5	StabEN_0.7	0.59	0.75	0.57	0.74
1.5	StabEN_0.8	0.52	0.67	0.50	0.65
1.5	StabEN_0.9	0.32	0.44	0.34	0.46
1.5	Jitter	0.61	0.78	0.50	0.68
2.0	Lasso	0.06	0.08	0.07	0.08
2.0	ENet	0.06	0.07	0.06	0.07
2.0	StabL_0.6	0.33	0.55	0.28	0.51
2.0	StabL_0.7	0.29	0.46	0.28	0.44
2.0	StabL_0.8	0.20	0.29	0.17	0.27
2.0	StabL_0.9	0.08	0.12	0.07	0.11
2.0	StabEN_0.6	0.32	0.55	0.29	0.53
2.0	StabEN_0.7	0.32	0.51	0.30	0.49
2.0	StabEN_0.8	0.25	0.37	0.23	0.35
2.0	StabEN_0.9	0.12	0.18	0.10	0.15
2.0	Jitter	0.32	0.56	0.19	0.46

Competing Interests

The authors declare that they have no conflict of interest.

Author Contributions Statement

Mahdi Nouraie was responsible for drafting the manuscript, the development of the research methodology and for writing the computer code used throughout. Samuel Muller and Houying Zhu provided critical feedback on the content of the manuscript, refining the clarity and scope of the manuscript and the computer code.

Data Availability

The rat microarray data can be obtained from the National Center for Biotechnology Information (NCBI) website at www.ncbi.nlm.nih.gov, under accession number GSE5680.

Acknowledgments

Mahdi Nouraie was supported by the Macquarie University Research Excellence Scholarship (20213605). Samuel Muller and Houying Zhu were supported by the Australian Research Council Discovery Project Grant (DP260100348).

References

- Meinshausen, N., Bühlmann, P.: Stability selection. *Journal of the Royal Statistical Society Series B: Statistical Methodology* **72**(4), 417–473 (2010)
- Müller, S., Welsh, A.H.: On Model Selection Curves. *International Statistical Review* **78**(2), 240–256 (2010)
- Shah, R.D., Samworth, R.J.: Variable selection with error control: another look at stability selection. *Journal of the Royal Statistical Society Series B: Statistical Methodology* **75**(1), 55–80 (2013)
- Nogueira, S., Sechidis, K., Brown, G.: On the Stability of Feature Selection Algorithms. *Journal of Machine Learning Research* **18**(174), 1–54 (2018)
- Wang, H., Lengerich, B.J., Aragam, B., Xing, E.P.: Precision Lasso: accounting for correlations and linear dependencies in high-dimensional genomic data. *Bioinformatics* **35**(7), 1181–1187 (2018)
- Soloff, J.A., Barber, R.F., Willett, R.: Bagging provides assumption-free stability. *Journal of Machine Learning Research* **25**(131), 1–35 (2024)
- Nouraie, M., Smith, C., Muller, S.: Bayesian stability selection and inference on selection probabilities. *Statistics and Computing* **36**(62) (2026)
- Shen, Z., Cui, P., Zhang, T., Kunag, K.: Stable learning via sample reweighting. *Proceedings of the AAAI Conference on Artificial Intelligence* **34**(04), 5692–5699 (2020)

- Zhang, X., Cui, P., Xu, R., Zhou, L., He, Y., Shen, Z.: Deep stable learning for out-of-distribution generalization. In: Proceedings of the IEEE/CVF Conference on Computer Vision and Pattern Recognition, pp. 5372–5382 (2021)
- Cui, P., Athey, S.: Stable learning establishes some common ground between causal inference and machine learning. *Nature Machine Intelligence* **4**, 110–115 (2022)
- Faletto, G., Bien, J.: Cluster Stability Selection. arXiv preprint arXiv:2201.00494 (2022)
- Nghiem, L.H., Byrd, M.C., Potgieter, C.J.: Estimation in linear errors-in-variables models with unknown error distribution. *Biometrika* **107**(4), 841–856 (2020)
- Nghiem, L.H., Potgieter, C.J.: A linear errors-in-variables model with unknown heteroscedastic measurement errors. arXiv preprint arXiv:2310.13874 (2023)
- Liu, C., Nghiem, L.: PhaseGMM: Phase-Function Based Estimation and Inference for Linear Errors-in-Variables (EIV) Models. (2026). R package version 0.1.0. <https://CRAN.R-project.org/package=PhaseGMM>
- Tibshirani, R.: Regression Shrinkage and Selection via the Lasso. *Journal of the Royal Statistical Society Series B: Statistical Methodology* **58**(1), 267–288 (1996)
- Zou, H., Hastie, T.: Regularization and variable selection via the elastic net. *Journal of the Royal Statistical Society Series B: Statistical Methodology* **67**(2), 301–320 (2005)
- Fan, J., Li, R.: Variable selection via nonconcave penalized likelihood and its oracle properties. *Journal of the American Statistical Association* **96**(456), 1348–1360 (2001)
- Wu, C.F.J.: Jackknife, Bootstrap and Other Resampling Methods in Regression Analysis. *The Annals of Statistics* **14**(4), 1261–1295 (1986)
- Breiman, L.: Random Forests. *Machine Learning* **45**, 5–32 (2001)
- Cannings, T.I., Samworth, R.J.: Random-projection ensemble classification. *Journal of the Royal Statistical Society Series B: Statistical Methodology* **79**(4), 959–1035 (2017)
- Pfister, N., Williams, E.G., Peters, J., Aebbersold, R., Bühlmann, P.: Stabilizing variable selection and regression. *The Annals of Applied Statistics* **15**(3), 1220–1246 (2021)
- Jeong, Y., Rothenhäusler, D.: Calibrated inference: Statistical inference that accounts for both sampling uncertainty and distributional uncertainty. *Journal of Machine Learning Research* **26**(196), 1–48 (2025)
- Shen, X., Bühlmann, P., Taeb, A.: Causality-oriented robustness: Exploiting general noise interventions. *Journal of the American Statistical Association* **0**(0), 1–12 (2026)
- Zhao, P., Yu, B.: On Model Selection Consistency of Lasso. *Journal of Machine Learning Research* **7**, 2541–2563 (2006)
- Meinshausen, N., Bühlmann, P.: High-dimensional graphs and variable selection with the Lasso. *The Annals of Statistics* **34**(3), 1436–1462 (2006)
- Bühlmann, P., Van De Geer, S.: *Statistics for High-Dimensional Data: Methods, Theory and Applications*. Springer, Berlin, Heidelberg (2011)
- Wieczorek, J., Lei, J.: Model selection properties of forward selection and sequential cross-validation for high-dimensional regression. *Canadian Journal of Statistics*

- 50**(2), 454–470 (2022)
- Takada, M., Suzuki, T., Fujisawa, H.: Independently Interpretable Lasso: A new regularizer for sparse regression with uncorrelated variables. In: Proceedings of the Twenty-First International Conference on Artificial Intelligence and Statistics. Proceedings of Machine Learning Research, vol. 84, pp. 454–463 (2018)
- Huang, M., Muller, S., Tarr, G.: Data-adaptive automatic threshold calibration for stability selection. *Journal of Statistical Computation and Simulation* **0**(0), 1–25 (2026)
- Scheetz, T.E., Kim, K.-Y.A., Swiderski, R.E., Philp, A.R., Braun, T.A., Knudtson, K.L., Dorrance, A.M., DiBona, G.F., Huang, J., Casavant, T.L., *et al.*: Regulation of gene expression in the mammalian eye and its relevance to eye disease. *Proceedings of the National Academy of Sciences* **103**(39), 14429–14434 (2006)
- Chiang, A.P., Beck, J.S., Yen, H.-J., Tayeh, M.K., Scheetz, T.E., Swiderski, R.E., Nishimura, D.Y., Braun, T.A., Kim, K.-Y.A., Huang, J., *et al.*: Homozygosity mapping with SNP arrays identifies TRIM32, an E3 ubiquitin ligase, as a Bardet–Biedl syndrome gene (BBS11). *Proceedings of the National Academy of Sciences* **103**(16), 6287–6292 (2006)
- Huang, J., Ma, S., Zhang, C.-H.: Adaptive Lasso for sparse high-dimensional regression models. *Statistica Sinica* **18**(4), 1603–1618 (2008)
- Vershynin, R.: *High-dimensional Probability: An Introduction with Applications in Data Science* vol. 47. Cambridge University Press, ??? (2018)
- Hoeffding, W.: Probability inequalities for sums of bounded random variables. *Journal of the American Statistical Association* **58**(301), 13–30 (1963)

Figure 1

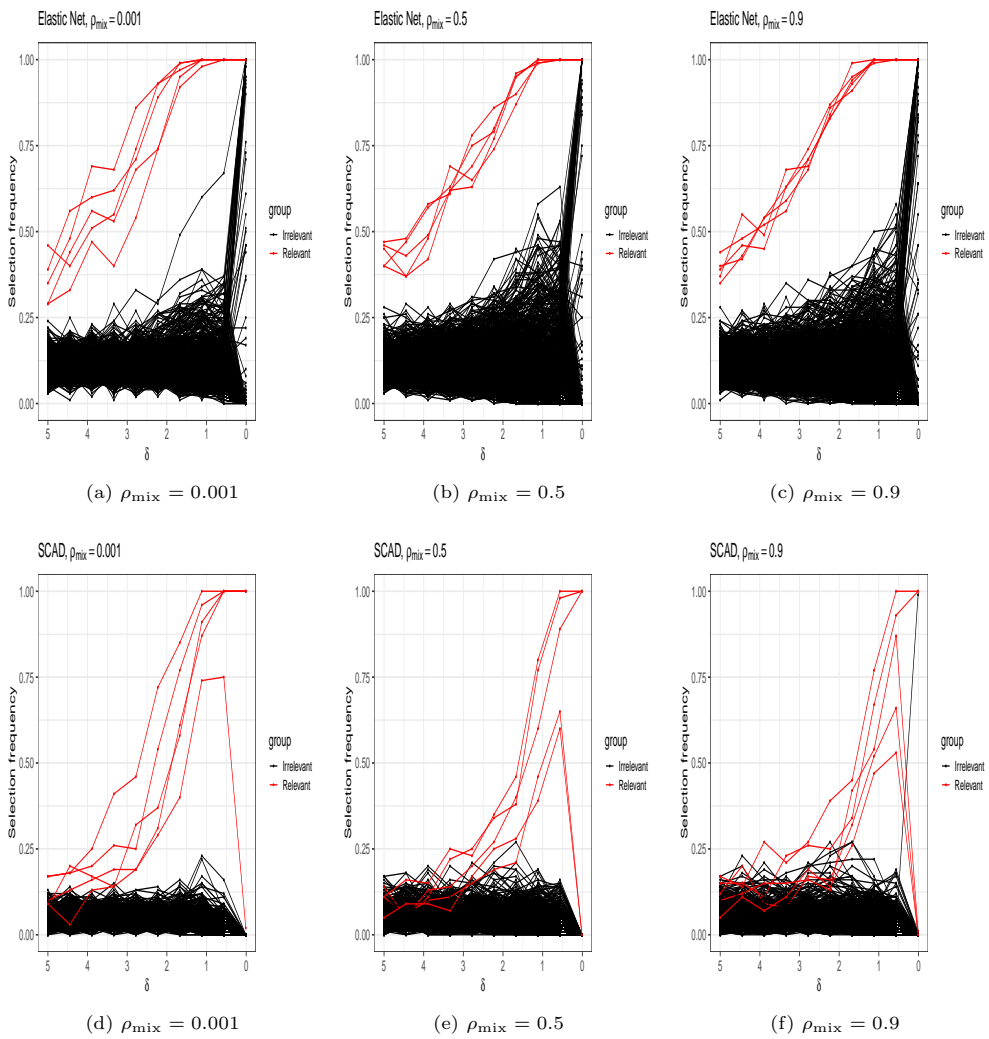


Fig. 1: Selection frequency of relevant (red) and irrelevant (black) features for ENet (first row) and SCAD (second row) under increasing design noise level δ

Theory Background

The Lasso is a standard regularization-based feature selection method that augments the least-squares loss with an ℓ_1 penalty to promote sparse coefficients. The estimator

is

$$\hat{\beta}(\lambda) = \arg \min_{\beta \in \mathbb{R}^p} \left(\frac{1}{2n} \|Y - X\beta\|_2^2 + \lambda \|\beta\|_1 \right),$$

where $\lambda \in \mathbb{R}^+$ denotes the Lasso regularization parameter. We focus on the Lasso because of its central role in feature selection and its well-studied selection consistency conditions. We first show that these conditions are robust to sufficiently small perturbations of the design matrix, which provides a theory-grounded basis for studying stability along a path of progressively increasing noise. Writing $X^{(\delta)} = X + W$ gives $\Sigma^{(\delta)} = \frac{1}{n} (X^{(\delta)})^\top X^{(\delta)} = \Sigma + \Delta$ with $\Delta = \frac{1}{n} (X^\top W + W^\top X + W^\top W)$. We treat the bound on Δ as a deterministic envelope: assume that

$$\|\Delta\|_\infty \leq C_1 \delta + C_2 \delta^2,$$

for constants $C_1, C_2 > 0$ depending on X . In the stochastic setting (Section 2.2), a corresponding bound will be established with high probability. Throughout, $\|\cdot\|_\infty$ denotes the induced matrix ℓ_∞ norm, i.e., the maximum absolute row sum. We also note that if $\max_{j,k} |A_{jk}| \leq t$, then $\|A\|_\infty \leq pt$. Throughout, $C, C_t, c_1 > 0$ denote absolute constants that may vary from line to line. A sharper control of $\|\Delta\|_\infty$ can be obtained via standard matrix concentration inequalities (e.g., matrix Bernstein), which avoid the conservative entrywise-to-row-sum scaling adopted here and yield dimension-dependent rates. We use $\Sigma^{(\delta)} = \frac{1}{n} (X^{(\delta)})^\top X^{(\delta)}$ in the deterministic analysis below. In the Gaussian setting, we instead consider the centered Gram (covariance) estimator

$$\tilde{\Sigma}^{(\delta)} = \frac{1}{n} (X^{(\delta)})^\top X^{(\delta)} - \delta^2 I_p,$$

which removes the bias induced by $W^\top W$. The matrix $\tilde{\Sigma}^{(\delta)}$ is an unbiased estimator of Σ , is symmetric, but is not necessarily positive semi-definite. The centering removes the leading bias of $W^\top W$; the remaining fluctuations are controlled in operator norm at the same order as the cross terms under standard Gaussian matrix concentration.

Proof of Lemma 1

Proof For $\delta \leq 1$, we may absorb the quadratic term and write

$$\|\Delta\|_\infty \leq (C_1 + C_2)\delta,$$

for a possibly larger constant. Write

$$\Sigma_{SS}^{(\delta)} = \Sigma_{SS} + \Delta_{SS}, \quad \Sigma_{S^cS}^{(\delta)} = \Sigma_{S^cS} + \Delta_{S^cS}.$$

Since the induced ℓ_∞ norm is the maximum absolute row sum, taking sub-matrices does not increase the norm. Hence

$$\|\Delta_{SS}\|_\infty \leq (C_1 + C_2)\delta, \quad \|\Delta_{S^cS}\|_\infty \leq (C_1 + C_2)\delta.$$

Step 1. Let $A = \Sigma_{SS}$ and $E = \Delta_{SS}$. If $\|A^{-1}\|_\infty \|E\|_\infty < 1$, then $A + E$ is invertible. This holds whenever $(C_1 + C_2)\|A^{-1}\|_\infty \delta < 1$. In that case,

$$\|(A + E)^{-1}\|_\infty \leq \frac{\|A^{-1}\|_\infty}{1 - \|A^{-1}\|_\infty \|E\|_\infty}.$$

Choose

$$\delta \leq \delta_1 := \frac{1}{2(C_1 + C_2)\|\Sigma_{SS}^{-1}\|_\infty},$$

so that $\|A^{-1}\|_\infty\|E\|_\infty \leq \frac{1}{2}$. Then

$$\|(\Sigma_{SS}^{(\delta)})^{-1}\|_\infty \leq 2\|\Sigma_{SS}^{-1}\|_\infty.$$

Using

$$(A + E)^{-1} - A^{-1} = -(A + E)^{-1}EA^{-1},$$

we obtain

$$\|(\Sigma_{SS}^{(\delta)})^{-1} - \Sigma_{SS}^{-1}\|_\infty \leq 2(C_1 + C_2)\|\Sigma_{SS}^{-1}\|_\infty^2 \delta.$$

Step 2.

$$\|\Delta_{S^c S}\|_\infty \leq (C_1 + C_2)\delta, \quad \|\Sigma_{S^c S}^{(\delta)}\|_\infty \leq \|\Sigma_{S^c S}\|_\infty + (C_1 + C_2)\delta.$$

Decompose

$$\begin{aligned} \Sigma_{S^c S}^{(\delta)}(\Sigma_{SS}^{(\delta)})^{-1} &= \Sigma_{S^c S}\Sigma_{SS}^{-1} + \Delta_{S^c S}\Sigma_{SS}^{-1} \\ &\quad + \Sigma_{S^c S}^{(\delta)}((\Sigma_{SS}^{(\delta)})^{-1} - \Sigma_{SS}^{-1}). \end{aligned}$$

Hence

$$\begin{aligned} \left\| \Sigma_{S^c S}^{(\delta)}(\Sigma_{SS}^{(\delta)})^{-1} - \Sigma_{S^c S}\Sigma_{SS}^{-1} \right\|_\infty &\leq (C_1 + C_2)\delta \left(\|\Sigma_{SS}^{-1}\|_\infty + 2\|\Sigma_{SS}^{-1}\|_\infty^2 \|\Sigma_{S^c S}\|_\infty \right) \\ &\quad + 2(C_1 + C_2)^2 \|\Sigma_{SS}^{-1}\|_\infty^2 \delta^2. \end{aligned}$$

Step 3. Combining the IC with Step 2 yields

$$\left\| \Sigma_{S^c S}^{(\delta)}(\Sigma_{SS}^{(\delta)})^{-1} \right\|_\infty \leq (1 - \eta) + a\delta + b\delta^2,$$

where

$$a = (C_1 + C_2) \left(\|\Sigma_{SS}^{-1}\|_\infty + 2\|\Sigma_{SS}^{-1}\|_\infty^2 \|\Sigma_{S^c S}\|_\infty \right), \quad b = 2(C_1 + C_2)^2 \|\Sigma_{SS}^{-1}\|_\infty^2.$$

Choose

$$\delta_0 := \min \left\{ \delta_1, \frac{\eta}{4a}, \sqrt{\frac{\eta}{4b}} \right\}.$$

Then for all $0 \leq \delta \leq \delta_0$,

$$a\delta + b\delta^2 \leq \frac{\eta}{2},$$

and therefore

$$\left\| \Sigma_{S^c S}^{(\delta)}(\Sigma_{SS}^{(\delta)})^{-1} \right\|_\infty \leq 1 - \frac{\eta}{2}.$$

□

Lemma 2: Statement and Proof

Lemma 2 (Product of independent Gaussians is sub-exponential) *Let $Z_1, Z_2 \sim \mathcal{N}(0, 1)$ be independent and set $U := Z_1 Z_2$. Then U is sub-exponential and $\|U\|_{\psi_1} \leq C_\psi$ for an absolute constant $C_\psi > 0$.*

Proof For $|t| < 1$,

$$\mathbb{E}(e^{tU}) = (1 - t^2)^{-1/2}, \quad \log \mathbb{E}(e^{tU}) = -\frac{1}{2} \log(1 - t^2).$$

Using $-\log(1 - x) \leq 2x$ for $|x| \leq 1/2$,

$$\log \mathbb{E}(e^{tU}) \leq t^2 \quad \text{for } |t| \leq 1/2.$$

Hence $\log \mathbb{E}(e^{tU}) \leq t^2$ for $|t| \leq 1/2$, which implies a local sub-Gaussian MGF bound. This in turn yields a finite ψ_1 -Orlicz norm, so U is sub-exponential with $\|U\|_{\psi_1} \leq C_\psi$. □

Proof of Theorem 1

Proof Let

$$L := \log \frac{4p^2}{\alpha}, \quad \Delta := \tilde{\Sigma}^{(\delta)} - \Sigma,$$

$$t_1 := 2M\sqrt{\frac{2\delta^2 L}{n}}, \quad t_2 := C_t \delta^2 \left(\sqrt{\frac{L}{n}} + \frac{L}{n} \right), \quad \varepsilon := p(t_1 + t_2).$$

Step 1: decomposition.

$$\Delta = \frac{1}{n}(X^\top W + W^\top X) + \left(\frac{1}{n}W^\top W - \delta^2 I_p \right) =: A + B.$$

Step 2: bound A. For each (j, k) ,

$$\left(\frac{1}{n}X^\top W \right)_{jk} \sim \mathcal{N}\left(0, \frac{\delta^2}{n^2} \sum_{i=1}^n X_{ij}^2\right), \quad \frac{\delta^2}{n^2} \sum_{i=1}^n X_{ij}^2 \leq \frac{\delta^2 M^2}{n}.$$

Thus

$$\mathbb{P}(|(X^\top W/n)_{jk}| > t_1) \leq 2 \exp\left(-\frac{nt_1^2}{2\delta^2 M^2}\right) \leq 2e^{-L}.$$

Union bound over p^2 entries:

$$\mathbb{P}\left(\max_{j,k} |(X^\top W/n)_{jk}| > t_1\right) \leq 2p^2 e^{-L} = \frac{\alpha}{2}.$$

Hence

$$\|A\|_\infty \leq p t_1 \quad \text{with probability at least } 1 - \frac{\alpha}{2}.$$

Step 3: bound B.

Diagonal.

$$\mathbb{P}(|B_{jj}| > t_2) \leq 2e^{-L}.$$

Off-diagonal. By sub-exponential Bernstein (see, e.g. [Vershynin \(2018\)](#)) and choice of C_t absorbing constants,

$$\mathbb{P}(|B_{jk}| > t_2) \leq 2e^{-L}.$$

Union bound.

$$\mathbb{P}\left(\max_{j,k} |B_{jk}| > t_2\right) \leq 2p^2 e^{-L} = \frac{\alpha}{2}.$$

Thus

$$\|B\|_\infty \leq p t_2 \quad \text{with probability at least } 1 - \frac{\alpha}{2}.$$

Step 4: combine. By union bound over Steps 2-3,

$$\|\Delta\|_\infty \leq p(t_1 + t_2)$$

with probability at least $1 - \alpha$.

Step 5: deterministic IC stability. On the event $\|\Delta\|_\infty \leq \varepsilon \leq \varepsilon_0$, Lemma 1 implies

$$\left\| \tilde{\Sigma}_{S^c S}^{(\delta)} (\tilde{\Sigma}_{SS}^{(\delta)})^{-1} \right\|_\infty \leq 1 - \frac{\eta}{2}.$$

Therefore the stated bound holds with probability at least $1 - \alpha$.

As is clear from the arguments, the same proof strategy extends to other feature selection methods whose consistency relies on comparable near-orthogonality conditions. \square

Proof of Theorem 2

Proof Fix $\delta \in \mathcal{G}$ and $j \in \{1, \dots, p\}$. Conditional on (X, Y) , the indicators $1\{\hat{\beta}_j^{(b, \delta)} \neq 0\}$ are i.i.d. Bernoulli with mean $f_j^{(\delta)}$. By Hoeffding's inequality (Hoeffding, 1963), for any $t > 0$,

$$\mathbb{P}\left(\left|\hat{f}_j^{(\delta)} - f_j^{(\delta)}\right| > t\right) \leq 2e^{-2Bt^2}.$$

Applying a union bound over all mp pairs (δ, j) gives

$$\mathbb{P}\left(\max_{\delta \in \mathcal{G}} \max_{1 \leq j \leq p} \left|\hat{f}_j^{(\delta)} - f_j^{(\delta)}\right| > \varepsilon\right) \leq 2mp e^{-2B\varepsilon^2} = \alpha,$$

with ε as defined. Hence, with probability at least $1 - \alpha$, for all $\delta \in \mathcal{G}$ and all j ,

$$\left|\hat{f}_j^{(\delta)} - f_j^{(\delta)}\right| \leq \varepsilon.$$

On this event, averaging preserves the same uniform deviation bound:

$$\left|\widehat{\bar{f}}_j - \bar{f}_j\right| = \left|\frac{1}{m} \sum_{\delta \in \mathcal{G}} (\hat{f}_j^{(\delta)} - f_j^{(\delta)})\right| \leq \frac{1}{m} \sum_{\delta \in \mathcal{G}} \left|\hat{f}_j^{(\delta)} - f_j^{(\delta)}\right| \leq \varepsilon.$$

Therefore,

$$\min_{j \in S} \widehat{\bar{f}}_j \geq \min_{j \in S} \bar{f}_j - \varepsilon, \quad \max_{k \in S^c} \widehat{\bar{f}}_k \leq \max_{k \in S^c} \bar{f}_k + \varepsilon.$$

By Assumption 1, $\min_{j \in S} \bar{f}_j \geq \max_{k \in S^c} \bar{f}_k + \gamma$, hence

$$\min_{j \in S} \widehat{\bar{f}}_j - \max_{k \in S^c} \widehat{\bar{f}}_k \geq \gamma - 2\varepsilon.$$

If $\varepsilon < \gamma/2$, then $\min_{j \in S} \widehat{\bar{f}}_j > \max_{k \in S^c} \widehat{\bar{f}}_k$, so any τ satisfying $\max_{k \in S^c} \widehat{\bar{f}}_k < \tau \leq \min_{j \in S} \widehat{\bar{f}}_j$ yields $\hat{S}(\tau) = S$. \square

Remarks

Remark 1 Beyond irrepresentability, Lasso support recovery also requires a *beta-min* condition,

$$\min_{j \in S} |\beta_j| \geq c_0,$$

for some $c_0 > 0$. Under perturbations, this introduces an additional restriction on the admissible noise level. In particular, since the Lasso estimation error typically increases with the perturbation magnitude, correct support recovery requires this error to be small relative to the minimal signal strength. Consequently, δ must be sufficiently small compared to c_0 so that the perturbation-induced error does not obscure the nonzero coefficients.

Remark 2 Let $X^{(\delta)} = X + E_\delta$, where $E_\delta \in \mathbb{R}^{n \times p}$ has i.i.d. entries with mean 0 and variance δ^2 , independent of X . Consider

$$Y = X\beta + \varepsilon, \quad \mathbb{E}(\varepsilon) = 0, \quad \text{Cov}(\varepsilon) = \sigma^2 I_n, \quad \varepsilon \perp (X, E_\delta).$$

Since $X = X^{(\delta)} - E_\delta$, we can rewrite

$$Y = X^{(\delta)}\beta + \tilde{\varepsilon}, \quad \tilde{\varepsilon} := \varepsilon - E_\delta\beta.$$

Then

$$\text{Cov}(\tilde{\varepsilon}) = \text{Cov}(\varepsilon) + \text{Cov}(E_\delta\beta) = \sigma^2 I_n + \delta^2 \|\beta\|_2^2 I_n = (\sigma^2 + \delta^2 \|\beta\|_2^2) I_n,$$

using independence across columns of E_δ within each row and independence from ε . This suggests an effective increase in noise level (in a heuristic sense), degrading the signal-to-noise ratio and tending to suppress selections under fixed tuning (e.g., fixed λ). This is the classical errors-in-variables effect, where treating $X^{(\delta)}$ as noise-free induces attenuation and loss of identifiability in high-noise regimes. Note that $\tilde{\varepsilon}$ is not independent of $X^{(\delta)}$, so this is not a standard homoscedastic regression model.

Remark 3 Our method increases computational cost by approximately $|\mathcal{G}|$ relative to Stability Selection, as it repeats the procedure across perturbation levels using full-sample fits rather than half-sample sub-sampling, trading higher computation for robustness under noise perturbations.

Algorithm

Algorithm 1 2D Stability Selection

- 1: **Input:** Data (X, Y) ; grid $\mathcal{G} = \{\delta_1, \dots, \delta_m\}$; number of replicates B
 - 2: **Input:** Base selector with fixed tuning parameters (e.g. fixed λ)
 - 3: **for** each $\delta \in \mathcal{G}$ **do**
 - 4: **for** $b = 1$ to B **do**
 - 5: Generate $W^{(b)}$ with i.i.d. $\mathcal{N}(0, \delta^2)$ entries
 - 6: Form $X^{(b, \delta)} = X + W^{(b)}$
 - 7: Fit selector to $(X^{(b, \delta)}, Y)$ to obtain $\hat{\beta}^{(b, \delta)}$
 - 8: **end for**
 - 9: Compute frequencies $\hat{f}_j^{(\delta)} = \frac{1}{B} \sum_{b=1}^B 1\{\hat{\beta}_j^{(b, \delta)} \neq 0\}$ for all j
 - 10: **end for**
 - 11: Compute δ -averaged frequencies $\hat{f}_j = \frac{1}{m} \sum_{\delta \in \mathcal{G}} \hat{f}_j^{(\delta)}$ for all j
 - 12: Sort $\{\hat{f}_j\}_{j=1}^p$ in decreasing order to obtain $\hat{f}_{(1)} \geq \dots \geq \hat{f}_{(p)}$
 - 13: Compute $\hat{s} = \arg \max_{1 \leq k < p} (\hat{f}_{(k)} - \hat{f}_{(k+1)})$
 - 14: Set $\hat{\tau} = \frac{1}{2} (\hat{f}_{(\hat{s})} + \hat{f}_{(\hat{s}+1)})$
 - 15: Let $\hat{S} = \{j : \hat{f}_j \geq \hat{\tau}\}$
 - 16: **return** \hat{S}
-